DOI: 10.31276/VJSTE.2024.0141

Structural distortion and temperature-dependent carrier transport of Al-, Ga-, and In-doped ZnO thin films

Trang Thuy Thi Phan[1, 2], Oanh Kieu Truong Le[1, 2], Hoa Thi Lai[2, 3], Quang Thua Trieu[1, 2], Thu Bao Nguyen Le[2, 4], Vinh Cao Tran[1, 2], Thang Bach Phan[1, 2, 3], Anh Tuan Thanh Pham[1, 2, 3*]

[1]Laboratory of Advanced Materials, University of Science, Vietnam National University - Ho Chi Minh City, 227 Nguyen Van Cu Street, Cho Quan Ward, Ho Chi Minh City, Vietnam
[2]Vietnam National University - Ho Chi Minh City, Linh Xuan Ward, Ho Chi Minh City, Vietnam
[3]Centre for Innovative Materials and Architectures, Linh Xuan Ward, Ho Chi Minh City, Vietnam
[4]Faculty of Applied Science, Ho Chi Minh University of Technology, 268 Ly Thuong Kiet Street, Dien Hong Ward, Ho Chi Minh City, Vietnam

Received 17 December 2024; revised 15 January 2025; accepted 4 February 2025

Abstract:

ZnO-based films hold significant potential for optoelectronic applications, such as transparent electrodes and absorbance layers, as well as thermoelectric applications. Doping with Al, Ga, and In has attracted considerable attention for controlling the carrier transport properties of these films. Pure ZnO, Al-doped ZnO, Ga-doped ZnO, and In-doped ZnO films, each with a similar doping ratio of 1 wt%, were successfully deposited on glass substrates using the magnetron sputtering technique. X-ray diffraction was employed to confirm the ZnO structure, while temperature-dependent Hall-effect measurements were utilised to investigate the dependence of carrier transport on temperature. The results indicate that Al and Ga dopants enhance conductivity more effectively than In. This may be attributed to a substantial increase in carrier concentration when Al and Ga are doped into ZnO-based films as the temperature rises. Conversely, the In-doped ZnO film exhibits an increase in mobility, resulting in enhanced conductivity. These findings underscore the intricate interplay between doping elements, measurement temperature, and the electrical behaviour in ZnO films, offering valuable insights for further optimisation and application in various electronic and optoelectronic devices. This research opens the possibility of controlling the properties of ZnO films for applications at different operating temperatures.

Keywords: **carrier transport, magnetron sputtering, structural distortion, temperature dependence, ZnO-based films.**

Classification numbers: **2.1. 2.3**

1. Introduction

For decades, transparent conductive oxides (TCOs) have been extensively researched, particularly for their application in photovoltaic devices. Various oxide materials such as SnO_2 [1], TiO_2 [2], and ZnO [3] have been explored for producing high-quality transparent conductive films. ZnO stands out due to its advantageous properties including a large band gap (3.36 eV), large exciton energy (60 meV), and environmental friendliness. However, one drawback of ZnO is its relatively poor electrical conductivity [4], prompting researchers worldwide to explore strategies for improvement. Doping has garnered significant attention, with many elements such as group IIIA (group 13) elements (Al, Ga, In) [5, 6], rare earth elements (Ta, La, Y) [7-9], and halogen elements (F, Cl) [10-12], being investigated for their potential to enhance the electrical properties of ZnO films. Among these, group IIIA elements are widely used for doping the ZnO matrix to enhance electrical conductivity. Various fabrication methods, including pulsed laser deposition (PLD) [13], DC magnetron sputtering [14], and the sol-gel method [15], have been employed to produce doped thin films, with magnetron sputtering being particularly notable for its ease of deposition parameter control and high uniformity. J.J. Ding, et al. (2009) [16] reported that Al-doped ZnO with a concentration of 3 wt% enhances crystallinity and optical properties. Other studies have demonstrated the effectiveness of doping Ga with a concentration of 5 wt%, showing improvements in the electrical properties [17]. C.E. Benouis, et al. (2010) [18] showed the enhancement in the electrical characteristics of IZO films with the doping ratio of 2 wt%. However, very few groups have studied the effects of low impurity concentrations on the structural, electrical, and optical changes of films doped with IIIA-group elements. Hence, this research aims to investigate variations in structural and optical characteristics, and particularly alterations in electrical properties dependent on measuring temperature, of group IIIA impurities at the same low doping concentration, specifically 1 wt%.

*Corresponding author: Email: pttanh@hcmus.edu.vn

2. Materials and methods

Zinc oxide (ZnO), aluminium-doped zinc oxide (AZO), gallium-doped zinc oxide (GZO), and indium-doped zinc oxide (IZO) thin films were deposited on glass substrates via DC magnetron sputtering using a Leybold Univex-450 system from self-produced 3-inch ceramic targets. The targets were produced from commercial oxide powders, including ZnO (Merck, 99.99%), Al_2O_3 (Merck, 99.99%), Ga_2O_3 (Sigma Aldrich, 99.99%), and In_2O_3 (Sigma Aldrich, 99.99%). The powders, including pure ZnO, ZnO+Al_2O_3, ZnO+Ga_2O_3, and ZnO+In_2O_3, were mixed at an atomic ratio of M:Zn=1:99 (doping ratio of 1 wt%), where M is Al, Ga, or In. The powder mixtures were wet ball-milled in distilled water for 5 hours with alumina grinding media. Subsequently, the mixtures were dried for a day at 120°C, cold-pressed, and sintered at 1400°C in air for 3 hours. The sintered targets were carefully polished and cleaned for the sputtering process. The sputtering process took place in a vacuum chamber filled with argon gas (4N), maintaining a sputtered pressure of 3.5 mTorr, a DC power of 60 W, a deposition temperature of 300°C, and a sputtering time of 20 minutes.

The film thickness was maintained at approximately 600 nm, controlled via in-situ deposition rate measurement using a quartz crystal oscillator (Inficon XTM/2). The structural characteristics of both pure ZnO and doped ZnO films were examined using X-ray diffraction analysis with a Bruker D8-Advance instrument. Electrical properties, including carrier concentration, mobility, and resistivity of the films, were assessed using Hall-effect-based measurements performed with a Linseis HCS-1 instrument employing the Van der Pauw method across temperatures ranging from 300 K to 773 K, under a magnetic field of 0.7 T. The optical transmittance of the films was evaluated using a UV-Vis spectrophotometer (Jasco V-770).

3. Results

The structural characteristics of both pure ZnO films and ZnO films doped with Al, Ga, and In were analysed using X-ray diffraction (XRD), as depicted in Fig. 1A. High-quality crystalline films exhibit a single distinct diffraction peak corresponding to the (002) lattice plane of ZnO, consistent with the standard reference (JCPDS 36-1451) [19]. This indicates that the films are oriented along the c-axis, which is common for sputter-deposited films [20]. Furthermore, there was no evidence of oxide-related phases from the dopants, suggesting that Al^{3+}, Ga^{3+}, and In^{3+} ions were integrated into the ZnO lattice either by substituting zinc atoms or occupying interstitial positions. To consider it, the (002) plane was magnified in Fig. 1B, and the crystallographic data of the films was calculated in Table 1.

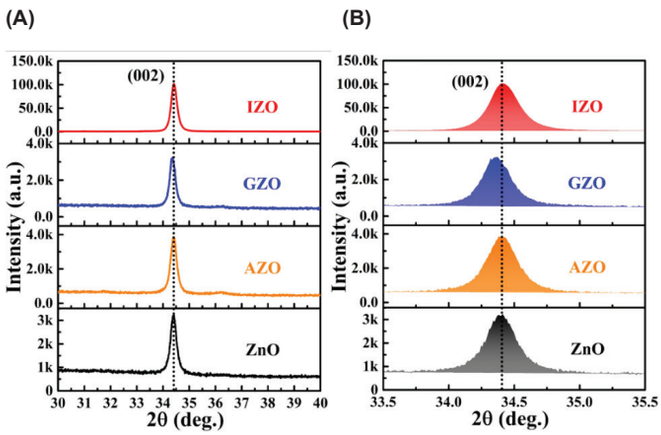

Fig. 1. (A) The overall X-ray diffraction pattern and (B) a magnified view of the 2θ angle range from 33.5° to 35.5° of the pure ZnO, AZO, GZO, and IZO films.

Table 1. Crystallographic characteristics of pure ZnO films and ZnO films doped with Al, Ga, and In.

Samples	2θ (deg.)	FWHM (deg.)	$d_{(002)}$ (nm)	c (nm)	ε	D (nm)
ZnO	34.41	0.267	0.2603	0.5206	0.0377	31.13
AZO	34.40	0.276	0.2604	0.5207	-0.0282	30.11
GZO	34.37	0.253	0.2606	0.5212	-0.2261	32.87
IZO	34.41	0.259	0.2603	0.5206	0.0377	32.07

The difference in ionic radius between the dopants and the host lattice can induce alterations in the residual stress within the films. Residual stress (ε) of the films can be estimated by using the formula [21]:

$$\varepsilon=[2C_{13}^2-C_{33}(C_{11}+C_{12})]/2C_{13}\times(c_f-c_o)/c_o$$

where C_{11}=208.8, C_{33}=213.8, C_{12}=119.7, and C_{13}=104.2 GPa are the elastic parameters for ZnO; c_o and c_f are the lattice constants of the stress-free ZnO and the films, respectively, as also shown in Table 1. The ZnO film displays tensile stress, a characteristic also observed in the In-doped ZnO film, suggesting a competition between the substitution and intercalation of indium within the ZnO lattice because of the large ionic radius of In^{3+} (0.081 nm) [22]. In contrast, both Al- and Ga-doped ZnO films show compressive stress, with Ga-doped ZnO displaying the highest compressive stress. This suggests the presence of Al^{3+} and Ga^{3+} impurities in the ZnO crystal lattice at interstitial sites because the ionic radius of Al^{3+} (0.053 nm) [23], and Ga^{3+} (0.062 nm) are smaller than that of ZnO.

To assess crystal quality further, the average crystal size was determined using the Scherrer function, given by $D=0.9\lambda/\beta\cos\theta$ [17], where λ is the CuKα X-ray wavelength, θ is the Bragg angle, and β is the full width at half maximum. The calculated D values for the films were found to be 31.13, 30.11, 32.87, and 32.07 nm for ZnO, AZO, GZO, and IZO,

respectively. These values show no significant difference, indicating that at a doping concentration of 1 wt%, group IIIA impurities do not distinctly influence grain size growth.

The carrier concentration, mobility, and resistivity of pure ZnO films and ZnO films doped with Al, Ga, and In according to measuring temperature are shown in Fig. 2. The pure ZnO film exhibits the highest resistivity due to its low carrier concentration and mobility, regardless of measuring temperature. Conversely, films doped with Al, Ga, and In demonstrate enhanced electrical conductivity compared to pure ZnO. Specifically, the improved conductivity observed in the IZO film is attributed to an increase in carrier concentration and a significant enhancement in mobility. This indicates that the presence of indium helps balance the lattice network, maintaining the tensile stress state and improving mobility in the film. This is in agreement with another study [24]. Conversely, both AZO and GZO films exhibit nearly identical conductivities, higher than IZO, primarily due to an increase in carrier concentration rather than mobility. Interestingly, the electrical conductivity trends of AZO and GZO films are similar, suggesting that compressive stress in the film enhances its electrical properties, specifically by increasing carrier concentration.

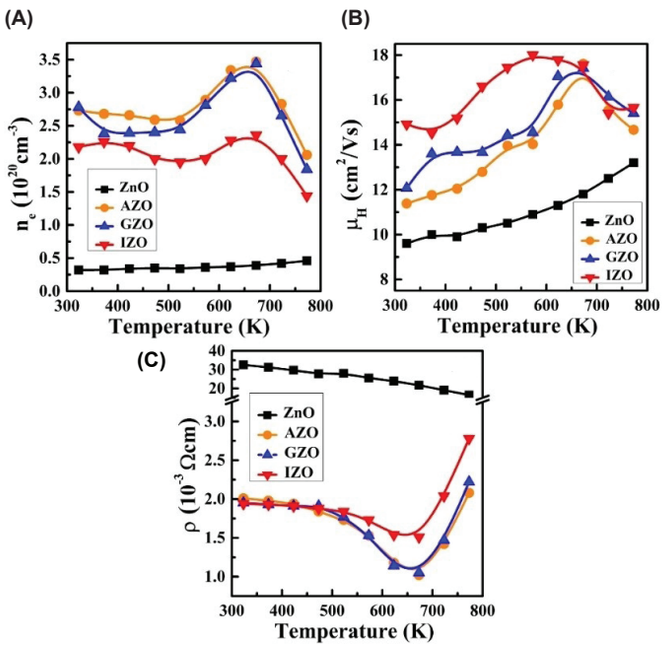

Fig. 2. Temperature dependence of electrical parameters: (A) Carrier concentration; **(B)** Mobility; **(C)** Resistivity of pure ZnO films and ZnO films doped with Al, Ga, and In.

UV-Vis spectroscopy was employed to examine the optical properties of both pure ZnO and doped ZnO films. In Fig. 3A, it is observed that both pure ZnO films and those doped with Al, Ga, and In elements exhibit moderate transmittance, surpassing 75% in the visible light region. This suggests that at a doping concentration of 1 wt%, the

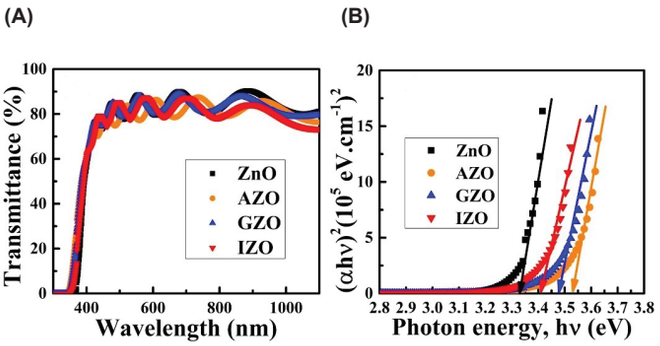

Fig. 3. (A) Transmittance spectra and (B) E_g bandgap of pure ZnO films and ZnO films doped with Al, Ga, and In.

transmittance does not significantly improve compared to pure ZnO films. Fig. 3B illustrates the measurement of the optical band gap (E_g) using the Tauc plot method to analyse the impact of impurities on the thin film's optical band gap value [25]. Using the following equation:

$$(\alpha h\nu)^2 = A\,(h\nu - E_g)$$

The Tauc plot method plots the value $(\alpha h\nu)^2$ against the photon energy ($h\nu$), where α represents the absorption coefficient and A is a constant dependent on the material's nature. The energy bandgap value is determined by extrapolating the straight-line portion of the curve to the point where the absorption coefficient is zero, providing the energy bandgap. The E_g values for the films were determined as 3.33 eV for pure ZnO, 3.40 eV for AZO, 3.47 eV for GZO, and 3.53 eV for IZO films, respectively. It is evident that the doped ZnO films tend to shift towards higher energies compared to the pure ZnO ones. This indicates a consistent pattern of E_g and carrier concentration, aligning with the Burstein-Moss effect [26].

4. Discussion

As shown in Fig. 1 and Table 1, the dopants do not influence the direction of film growth, yet there is a variation in the intensity of the (002) peak among the differently doped films. The increase in the intensity of the (002) peak in the doped ZnO films is observed, with the highest crystalline enhancement for the In-doped ZnO film. This demonstrates that doping with group IIIA elements does not alter the growth direction (002) but enhances crystal quality. Notably, with the same doping ratio of 1%, the IZO film exhibits a greater improvement in crystal quality compared to AZO and GZO films. Furthermore, the variation in radius between the dopant and the lattice results in alterations in the 2θ angle and full width at half maximum (FWHM) of the doped ZnO film. To facilitate the observation of this alteration, an angular range from 33.5 to 35.5° for 2θ was explored, alongside the calculation of crystallographic parameters of the films. Initially, there is no alteration in the 2θ angle towards higher or lower values observed in pure ZnO

and In-doped ZnO. Additionally, the 2θ angle of the AZO film exhibits a minimal deviation in comparison to the 2θ angle of pure ZnO, emphasising the good crystalline quality of AZO and IZO films. According to the previous study [27], doping with a concentration of 2 wt% of aluminium exhibited the phenomenon of shifting the diffraction peak (002). However, in our study, the doping concentration of aluminium and indium (1 wt%) was insufficient to cause a shift in the (002) peak, but it was adequate to enhance the crystal quality. The 2θ angle of Ga-doped ZnO exhibits a significant leftward deviation compared to the pure ZnO film. Typically, when gallium is doped, it would shift to the right of 2θ of ZnO, corresponding to a decrease in the lattice constant *c* [28]. However, the 2θ angle of this GZO film demonstrates the opposite behaviour, indicating that the presence of interstitial Ga in the ZnO network is predominant rather than substituting. The FWHM of GZO and IZO films is narrower than that of ZnO film, indicating excellent crystalline quality. Conversely, the FWHM of the AZO film increased slightly but remained very small and negligible.

The changes in carrier concentration (n_e), mobility (μ_H), and resistivity (ρ) are observed in ZnO and doped ZnO films across varying measuring temperature, as shown in Fig. 2. From 323 to 773 K, the carrier concentration in the ZnO film slightly increases, whereas the mobility increases rapidly, resulting in a gradual decrease in resistivity with temperature. This also shows that the pure ZnO film does not exhibit the typical degeneracy of semiconductors, with μ_H increasing due to thermal activation. For doped films, from 323 to 523 K, the carrier concentration of Al, Ga, and In-doped ZnO remains relatively stable, while mobility experiences a slight increase, leading to equivalent resistivity among these films. However, from 523 to 673 K, both Al and Ga-doped ZnO films exhibit an increase in both carrier concentration and mobility, with a significant rise in carrier concentration contributing to reduced resistivity. This suggests a substantial influence of carrier concentration on the temperature-dependent resistivity of AZO and GZO films. Additionally, the IZO film also demonstrates an increase in n_e and μ_H, with μ_H experiencing a rapid increase, considered the primary factor contributing to decreased resistivity with temperature. The increased carrier concentration in these films is contributed by oxidation within this temperature range, where free carriers emerge from the substitution of zinc ions with impurity ions and oxygen vacancies [29]. The increase in mobility is attributed to electron scattering on ionised impurities and predominant discharge defects causing transport disruptions in the film [30]. Between 673 and 773 K, the resistivity of doped ZnO starts increasing again due to a sharp decrease in carrier concentration and mobility, indicating metal-like degeneration properties in these films.

5. Conclusions

In conclusion, this study successfully deposited pure ZnO, AZO, GZO, and IZO films, where each film was doped with a dopant ratio of 1 wt% using the magnetron sputtering method. Significant variations in structural, electrical, and optical properties were observed among these ZnO films doped with different group IIIA elements. Notably, the electrical properties of the doped ZnO films were found to be closely linked to the measuring temperature, as revealed by Hall effect measurements. Specifically, the presence of Al and Ga impurities led to enhanced conductivity, primarily driven by a notable increase in carrier concentration with rising measuring temperature. In contrast, IZO films exhibited heightened mobility, resulting in increased conductivity. These findings underscore the intricate interplay between doping elements, measuring temperature, and the electrical behaviour in ZnO films, offering valuable insights for further optimisation and application in various electronic and optoelectronic devices.

CRediT author statement

Trang Thuy Thi Phan: Investigation, Formal analysis, Original draft preparation; Oanh Kieu Truong Le: Data curation, Investigation; Hoa Thi Lai: Data curation; Quang Thua Trieu: Data curation; Thu Bao Nguyen Le: Data curation; Vinh Cao Tran: Validation, Resources; Thang Bach Phan: Methodology, Resources, Funding acquisition; Anh Tuan Thanh Pham: Conceptualisation, Data curation, Supervision, Writing - Reviewing and Editing.

ACKNOWLEDGEMENTS

This research is funded by the National Foundation of Science and Technology Development of Vietnam (NAFOSTED) under the grant number 103.02-2021.54.

COMPETING INTERESTS

The authors declare that there is no conflict of interest regarding the publication of this article.

REFERENCES

[1] G. Giusti, V. Consonni, E. Puyoo, et al. (2014), "High performance ZnO-SnO_2:F nanocomposite transparent electrodes for energy applications", *ACS Appl. Mater. Interfaces*, **6(6)**, pp.14096-14107, DOI: 10.1021/am5034473.

[2] X. Wang, Z. Li, W. Xu, et al. (2015), "TiO_2 nanotube arrays based flexible perovskite solar cells with transparent carbon nanotube electrode", *Nano Energy*, **11**, pp.728-735, DOI: 10.1016/j.nanoen.2014.11.042.

[3] S. Tabassum, E. Yamasue, H. Okumura, et al. (2016), "Electrical stability of Al-doped ZnO transparent electrode prepared by sol-gel method", *Appl. Surf. Sci.*, **377**, pp.355-360, DOI: 10.1016/j.apsusc.2016.03.133.

[4] D.K. Sharma, S. Shukla, K.K. Sharma, et al. (2022), "A review on ZnO: Fundamental properties and applications", *Mater. Today Proc.*, **49**, pp.3028-3035, DOI: 10.1016/j.matpr.2020.10.238.

[5] P. Sikam, P. Moontragoon, Z. Ikonic, et al. (2019), "The study of structural, morphological and optical properties of (Al, Ga)-doped ZnO: DFT and experimental approaches", *Appl. Surf. Sci.*, **480**, pp.621-635, DOI: 10.1016/j.apsusc.2019.02.255.

[6] A. Tubtimtae, M.W. Lee (2012), "ZnO nanorods on undoped and indium-doped ZnO thin films as a TCO layer on nonconductive glass for dye-sensitized solar cells", *Superlattices Microstruct.*, **52(5)**, pp.987-996, DOI: 10.1016/j.spmi.2012.08.002.

[7] R. Zamiri, A.F. Lemos, A. Reblo, et al. (2014), "Effects of rare-earth (Er, La and Yb) doping on morphology and structure properties of ZnO nanostructures prepared by wet chemical method", *Ceram. Int.*, **40(1)**, pp.523-529, DOI: 10.1016/j.ceramint.2013.06.034.

[8] Y. Wu, C. Li, M. Li, et al. (2016), "Microstructural and optical properties of Ta-doped ZnO films prepared by radio frequency magnetron sputtering", *Ceram. Int.*, **42(9)**, pp.10847-10853, DOI: 10.1016/j.ceramint.2016.03.214.

[9] M. Thirumoorthi, J.T.J. Prakash (2015), "Structural, morphological characteristics and optical properties of Y doped ZnO thin films by sol-gel spin coating method", *Superlattices Microstruct.*, **85**, pp.237-247, DOI: 10.1016/j.spmi.2015.05.005.

[10] A.A. Galil, M.S.A. Hussien, I.S. Yahia (2021), "Synthesis and optical analysis of nanostructured F-doped ZnO thin films by spray pyrolysis: Transparent electrode for photocatalytic applications", *Opt. Mater. (Amst)*, **114**, DOI: 10.1016/j.optmat.2021.110894.

[11] E. Chikoidze, M. Nolan, M. Modreanu, et al. (2008), "Effect of chlorine doping on electrical and optical properties of ZnO thin films", *Thin Solid Films*, **516(22)**, pp.8146-8149, DOI: 10.1016/j.tsf.2008.04.076.

[12] Y. Larbah, B. Rahal, M. Adnane (2020), "The effect of fluorine doping on the properties of SnO_2 thin films deposited using spray pyrolysis method", *J. Optoelectron. Adv. Mater.*, **22(9-10)**, pp.518-522.

[13] V. Kumar, S.K. Singh, H. Sharma, et al. (2019), "Investigation of structural and optical properties of ZnO thin films of different thickness grown by pulsed laser deposition method", *Phys. B Condens. Matter*, **552**, pp.221-226, DOI: 10.1016/j.physb.2018.10.004.

[14] M.R.A. Cruz, O.C. Sanchez, E.L. Hipólito, et al. (2018), "ZnO thin films deposited by RF magnetron sputtering: Effects of the annealing and atmosphere conditions on the photocatalytic hydrogen production", *Int. J. Hydrogen Energy*, **43(22)**, pp.10301-10310, DOI: 10.1016/j.ijhydene.2018.04.054.

[15] D. Akcan, A. Gungor, L. Arda (2018), "Structural and optical properties of Na-doped ZnO films", *J. Mol. Struct.*, **1161**, pp.299-305, DOI: 10.1016/j.molstruc.2018.02.058.

[16] J.J. Ding, S.Y. Ma, H.X. Chen, et al. (2009), "Influence of Al-doping on the structure and optical properties of ZnO films", *Phys. B Condens. Matter*, **404(16)**, pp.2439-2443, DOI: 10.1016/j.physb.2009.05.006.

[17] J. Yang, Y. Jiang, L. Li, et al. (2017), "Structural, morphological, optical and electrical properties of Ga-doped ZnO transparent conducting thin films", *Appl. Surf. Sci.*, **421**, pp.446-452, DOI: 10.1016/j.apsusc.2016.10.079.

[18] C.E. Benouis, M. Benhaliliba, A.S. Juarez, et al. (2010), "The effect of indium doping on structural, electrical conductivity, photoconductivity and density of states properties of ZnO films", *J. Alloys Compd.*, **490(1-2)**, pp.62-67, DOI: 10.1016/j.jallcom.2009.10.098.

[19] B. Rahal, B. Boudine, Y. Larbah, et al. (2021), "Influence of low Cd-doping concentration (0.5 and 3 wt.%) and different substrate types (glass and silicon) on the properties of dip-coated nanostructured ZnO semiconductors thin films", *J. Inorg. Organomet. Polym. Mater.*, **31(10)**, pp.4001-4017, DOI: 10.1007/s10904-021-02024-y.

[20] Z. Onuk, N. Rujisamphan, R. Murray, et al. (2017), "Controllable growth and characterization of highly aligned ZnO nanocolumnar thin films", *Appl. Surf. Sci.*, **396**, pp.1458-1465, DOI: 10.1016/j.apsusc.2016.11.190.

[21] D.C. Truong, S. Thaowonkaew, P. Muthitamongkol, et al. (2022), "Relaxation of residual stress-controlled thermopower factor in transparent-flexible Ti-doped ZnO thin films", *Ceram. Int.*, **48(2)**, pp.2605-2613, DOI: 10.1016/j.ceramint.2021.10.043.

[22] Y. Li, R. Wang, Y. Li, et al. (2021), "First-principles calculation of photoelectric property in upconversion materials through In^{3+} doping", *J. Chem. Inf. Model.*, **61(2)**, pp.881-890, DOI: 10.1021/acs.jcim.0c01487.

[23] O. Marin, T. Soliz, J.A. Gutierrez, et al. (2019), "Structural, optical and vibrational properties of ZnO:M (M=Al^{3+} and Sr^{2+}) nano and micropowders grown by hydrothermal synthesis", *J. Alloys Compd.*, **789**, pp.56-65, DOI: 10.1016/j.jallcom.2019.03.115.

[24] X. Zhang, H. Lee, J.H. Kwon, et al. (2017), "Low-concentration indium doping in solution-processed zinc oxide films for thin-film transistors", *Materials (Basel)*, **10(8)**, DOI: 10.3390/ma10080880.

[25] Y. Cheng, K. Yang, J. Chen, et al. (2017), "Influence of substrate temperature on the optical properties of Sb-doped ZnO films prepared by MOCVD", *J. Mater. Sci. Mater. Electron.*, **28(3)**, pp.2602-2606, DOI: 10.1007/s10854-016-5836-z.

[26] M. Popa, L.C. Pop, G. Schmerber, et al. (2021), "Impact of the structural properties of holmium doped ZnO thin films grown by sol-gel method on their optical properties", *Appl. Surf. Sci.*, **562**, DOI: 10.1016/j.apsusc.2021.150159.

[27] O.M. Abdulmunem, M.J.M. Ali, E.S. Hassan (2020), "Optical and structural characterization of aluminium doped zinc oxide thin films prepared by thermal evaporation system", *Opt. Mater. (Amst).*, **109**, DOI: 10.1016/j.optmat.2020.110374.

[28] T. Ivanova, A. Harizanova, T. Koutzarova, et al. (2020), "Structural and optical characterization of nitrogen and gallium co-doped ZnO thin films deposited by sol-gel method", *J. Mol. Struct.*, **1206**, DOI: 10.1016/j.molstruc.2020.127773.

[29] V. Gurylev, T.P. Perng (2021), "Defect engineering of ZnO: Review on oxygen and zinc vacancies", *J. Eur. Ceram. Soc.*, **41(10)**, pp.4977-4996, DOI: 10.1016/j.jeurceramsoc.2021.03.031.

[30] A. Singh, S. Chaudhary, D.K. Pandya (2014), "On the temperature dependence of mobility in hydrogenated indium-doped ZnO thin films", *Acta Mater.*, **77**, pp.125-132, DOI: 10.1016/j.actamat.2014.05.048.